



LAWRENCE
LIVERMORE
NATIONAL
LABORATORY

Intra-Jet Shocks in Two Counter-Streaming, Weakly Collisional Plasma Jets

D. D. Ryutov, N. L. Kugland, H. S. Park, C.
Plechaty, B. A. Remington, J. S. Ross

April 20, 2012

The Physics of Plasmas

Disclaimer

This document was prepared as an account of work sponsored by an agency of the United States government. Neither the United States government nor Lawrence Livermore National Security, LLC, nor any of their employees makes any warranty, expressed or implied, or assumes any legal liability or responsibility for the accuracy, completeness, or usefulness of any information, apparatus, product, or process disclosed, or represents that its use would not infringe privately owned rights. Reference herein to any specific commercial product, process, or service by trade name, trademark, manufacturer, or otherwise does not necessarily constitute or imply its endorsement, recommendation, or favoring by the United States government or Lawrence Livermore National Security, LLC. The views and opinions of authors expressed herein do not necessarily state or reflect those of the United States government or Lawrence Livermore National Security, LLC, and shall not be used for advertising or product endorsement purposes.

Intra-jet shocks in two counter-streaming, weakly collisional plasma jets

D.D. Ryutov, N.L. Kugland, H.-S. Park, C. Plechaty, B.A. Remington, J.S. Ross

Lawrence Livermore National Laboratory, Livermore, CA 94551

Abstract

Counterstreaming laser-generated plasma jets can serve as a test-bed for the studies of a variety of astrophysical phenomena, including collisionless shock waves. In the latter problem, the jet's parameters have to be chosen in such a way as to make the collisions between the particles of one jet with the particles of the other jet very rare. This can be achieved by making the jet velocities high and the Coulomb cross-sections correspondingly low. On the other hand, the intra-jet collisions for high-Mach-number jets can still be very frequent, as they are determined by the much lower thermal velocities of the particles of each jet. This paper describes some peculiar properties of intra-jet hydrodynamics in such a setting: the steepening of smooth perturbations and shock formation affected by the presence of the "stiff" opposite flow; the role of a rapid electron heating in shock formation; ion heating by the intrajet shock. The latter effect can cause rapid ion heating which is consistent with recent counterstreaming jet experiments by J.S. Ross et al (Phys. Plas., **19**, 056501, 2012).

This brief communication is concerned with effects occurring in two laser-generated interpenetrating plasma jets in the geometry of Fig. 1. Such (or similar) geometry is used in the experiments on collisionless shocks [1-4] of relevance to astrophysics (see Refs. 5-7 and further astrophysical references therein).

By design, the ion kinetic energy of the interpenetrating jets is high, so as to make Coulomb collisions between the ions of the two jets negligible and allow for the studies of collisionless interactions, if the latter are strong enough. Such a plasma has been characterized in much detail by Thomson scattering in Ref. [8].

The interpenetrating jets have very high Mach number, i.e., the ion temperature within each jet is much less than the ion directed energy. This means that the collisions between the ions of the same jet are much more frequent than those between the ions of two jets. To provide some numerical guidance, we present Table 1 for the conditions typical for the aforementioned experiments [1, 8]. One sees that the intra-jet collisional mean-free path is very short, meaning that each jet is a highly collisional entity, describable hydrodynamically.

In our paper we study intra-jet hydrodynamic motions, with an emphasis on intra-jet collisional shocks. This allows us to suggest a plausible mechanism of rapid ion heating observed in the experiment [8]. We consider purely classical hydrodynamical effects and do not include collisionless interactions. Our model, therefore, serves as a background for the possible analysis of microturbulence and collisionless effects, if they are present.

An interesting feature of the hydrodynamic motions in a single jet is the presence of a “stiff” background ion population provided by the second, counterstreaming jet. This

background is “stiff” in the sense that the electric fields produced by the hydrodynamic motions in the first jet have only a small effect on the counterpropagating ions, which have very high energy in the rest-frame of the first jet. So, the ions of the second jet can be considered as a known background, with the density being a given function of space and time, $n^*(\mathbf{r},t)$, and not affected by the motions in the first jet. The electron thermal velocity is orders of magnitude higher than the relative velocity of the jets. Therefore, electron population is common and can be characterized by a single density n_e and temperature T_e .

In the plasma with parameters mentioned in Table 1, the Debye radius is smaller than all other scales, meaning that the plasma is quasineutral. The quasineutrality constraint can be represented as

$$n_i + n^* = n_e / Z \tag{1}$$

We remind that collisions between the ions of the two jets are very rare and can be neglected. They play some role in a weak ion heating by the small-angle scattering, which we mention later, but not in the dynamics of the first jet.

The Thomson scattering measurements [8] have shown that, when a substantial overlapping of the jets occurs, the electron temperature rapidly (within a fraction of the ion transit time) increases from the initial value below 100 eV to values of order of 1 keV. Purely collisional effect of the ion drag vs. the electrons [9] is sufficient to account for the rapid electron heating. With that, the relative energy decrease of the ion jets is still small, $\sim 10\%$ [8], i.e., the model of freely expanding interpenetrating jets remains valid.

The ions of each jet are heated by a small-angle scattering on the ions of the opposite jet. This leads to some ion heating, but the effect is a few times weaker than that

observed experimentally, ~ 0.3 keV vs 1.5 keV [8]. The processes discussed in our paper may be a contributor to the actually observed ion heating rate.

Another important feature of the experiment with counterstreaming jets is high electron thermal diffusivity. According to Ref. [10], it is

$$\chi_e (cm^2 / s) \approx 3.7 \cdot 10^{20} T_e^{5/2} (eV) / Z n_e (cm^{-3}) \quad (2)$$

(we have taken the Coulomb logarithm to be equal to 10). As a characteristic scale for further estimates we use the length $\ell = 1mm$, of order of the jet radius in experiments [1, 8], see Fig. 1. Then, evaluating the heat conduction time over the characteristic scale of $\ell = 1mm$ as $\tau_\chi = \ell^2 / 2\chi_e$, one obtains the time mentioned in Table 1: this time is short compared to other characteristic times. Actually, for higher electron temperatures approaching 1 keV, the electron mean-free path becomes just a few times less than the scale-length and the heat conduction model with the diffusivity (2) breaks down (e.g., [11] and references therein): the electrons fly over the scale ℓ experiencing just a few scattering events, and form one Maxwell-Boltzmann population over the length exceeding ℓ . Note that the electron-electron collisions are very frequent (Table 1), so that electron distribution is indeed close to a Maxwell-Boltzmann distribution. The electron density is then related to the electrostatic potential by Boltzmann relation: $T_e \nabla n_e = e n_e \nabla \varphi$.

When making numerical estimates, we use the following set of plasma parameters:

$$n_i = n^* = 10^{18} \text{ cm}^{-3}; u = 10^8 \text{ cm/s}; Z = 6 \text{ (carbon)}, \quad (3)$$

where u is a velocity of a jet (so that the relative velocity is $2u$). The jet crossing time $\tau_u = \ell / u$ over the scale $\ell = 1mm$, is $\sim 10^{-9}$ s, longer than the heat conduction time τ_χ and/or electron-electron collision time τ_{ee} .

The set of hydrodynamic equations for a uniform T_e becomes:

$$m_i n_i \frac{d\mathbf{v}_i}{dt} = -\nabla p_i - e Z n_i \nabla \varphi \quad (4)$$

$$\frac{dn_i}{dt} + n_i \nabla \cdot \mathbf{v}_i = 0 \quad (5)$$

$$\nabla \varphi = \frac{T_e}{e} \frac{\nabla(n_i + n^*)}{n_i + n^*} \quad (6)$$

$$p_i = n_i T_i \quad (7)$$

$$\frac{dT_i}{dt} + \frac{2}{3} T_i \nabla \cdot \mathbf{v}_i = 0 \quad (8)$$

where $d/dt \equiv \partial/\partial t + \mathbf{v}_i \cdot \nabla$ and we accounted for Eq. (1). The presence of the ion background enters the problem via Eq. (6).

We start from considering basic features of the hydrodynamic equations for a uniform and constant in time background n^* and then proceed to include effects associated with the variation of n^* . We emphasize that we use the coordinate frame co-moving with the jet 1, i.e. the unperturbed state is that of a resting plasma. Consider the acoustic (linear) perturbations. By linearizing Eqs. (4)-(8) around the unperturbed uniform state, one obtains the following set:

$$m_i n_i \frac{\partial \delta \mathbf{v}_i}{\partial t} = -\nabla \delta p_i - e Z n_i \nabla \delta \varphi \quad (9)$$

$$\frac{\partial \delta n_i}{\partial t} + n_i \nabla \cdot \delta \mathbf{v}_i = 0 \quad (10)$$

$$\nabla \delta \varphi = \frac{T_e}{e} \frac{\nabla \delta n_i}{n_i + n^*} \quad (11)$$

$$\delta p_i = \frac{5}{3} p_i \frac{\delta n_i}{n_i} \quad (12)$$

The prefix δ is used to denote the perturbation; the quantities without this prefix are the unperturbed quantities. By expressing δp_i and $\delta \varphi$ in terms of δn_i from the last two equations, taking the divergence of the first equation, and substituting in it $\nabla \cdot \delta \mathbf{v}_i$ from the second equation, one finds a standard equation for the acoustic waves,

$$\frac{\partial^2 \delta n_i}{\partial t^2} = s^2 \nabla^2 \delta n_i, \quad (13)$$

with s being a sound speed expressed as:

$$s^2 = \frac{5}{3} \frac{p_i}{m n_i} + \frac{Z T_e}{m_i} \frac{n_i}{n_i + n^*} \quad (14)$$

One sees that the presence of an ion background leads to a decrease of the sound speed compared to the plasma of a single jet.

Now we consider shocks in the jet. The Rankine-Hugoniot relations across the shock front for the case of electrons with a uniform temperature (not varying across the shock due to their very high thermal conductivity) read as:

$$n_2 v_{x2} = n_1 v_{x1} \quad (15)$$

$$m_i n_{i2} v_{x2}^2 + p_{2i} + Z T_e n_{i2} = m_i n_{i1} v_{x1}^2 + p_{1i} + Z T_e n_{i1} + Z T_e n^* \ln \frac{n_{i2} + n^*}{n_{i1} + n^*} \quad (16)$$

$$\frac{m_i n_{i2} v_{x2}^3}{2} + \frac{\gamma v_{x2} p_{2i}}{\gamma - 1} + Z e \varphi_2 n_{i2} v_{x2} = \frac{m_i n_{i1} v_{x1}^3}{2} + \frac{\gamma v_{x1} p_{1i}}{\gamma - 1} + Z e \varphi_1 n_{i1} v_{x1}; \varphi_2 - \varphi_1 = \frac{T_e}{e} \ln \frac{n_{i2} + n^*}{n_{i1} + n^*} \quad (17)$$

where the subscripts “1” and “2” relate to the pre-shock and post-shock ions. These equations describe the continuity of the ion mass, momentum and energy fluxes across the shock interface. The shock thickness is of order of the ion mean-free-path with

respect to the intra-jet collisions, i.e., in the range of 10 μm (Table 1). The background ion density n^* provided by the other jet is not perturbed. The origin of the shocks and their effect on the ion heating will be discussed shortly.

To illustrate the effect of the ion heating by the shock, we consider the case where the pre-shock ion temperature is much smaller than the electron temperature, so that the terms containing p_{ii} in Eqs. (16) and (17) can be neglected. This assumption corresponds to the situation where the electrons have been rapidly heated by the aforementioned drag effect on the background of the cold ions. The dependence of the compression ratio and the post-shock ion temperature vs. the Mach number is presented in Figs. 2, 3. We define the Mach number as $M^2 = v_1^2 / s^2$, where s is defined by Eq. (14) with $p_I=0$. The relative density of the background ions (the stiff ions provided by the second jet) is characterized by the parameter $N=n_I/n^*$.

The shocks are formed from initially smooth density distribution by a familiar overtaking mechanism [12, 13]. The mechanism is associated with the fact that those parts of the Riemann wave that have higher density have also a higher propagation velocity and “overtake” the slower-moving part within the time of order of

$$\tau_{\text{overtake}} \sim \ell / s. \quad (18)$$

We speak here of the modestly nonlinear perturbations, with the density variation of order one. For strong perturbations, the overtaking occurs earlier, for weak perturbations, later.

The density variations are naturally present in the jet in the form of a radial density profile, with the density decreasing from the axis to the periphery at the distance $\sim \ell$. The related expansion dynamics would lead to formation of the radially-propagating

shocks. The non-uniformities can also be created by temporal variation of the laser intensity and resulting variations of the ablation rate. These non-uniformities are advected along the jet, gradually evolving into shocks.

However, all these processes are in some sense “frozen” until the rapid heating of the electrons occur: evolution of smooth perturbations in shocks takes long time in a cold plasma, as the sound speed is low. Also, if the electrons are cold, as they are before the onset of a fast heating, the post-shock ion temperature remains low.

The situation changes dramatically after a rapid electron heating. First, the duration (18) of the shock formation process rapidly falls into 1 ns range for $T_e \sim 1$ keV electrons. That is, even if the density variations at the time of a rapid electron heating were smooth, the shocks would be formed within ~ 1 ns time after the heating occurred. If the shocks in a cold plasma have already existed, then the rapid electron heating would lead to their transformation in much faster shocks. More importantly, the shocks of even modest intensity, with a Mach number of ~ 1.5 , would lead to a rapid ion heating, which would occur within the shock crossing time (1-2 ns for a shock with the Mach number 1.5-2). The resulting ion temperature would exceed the electron temperature for even relatively weak shocks, with the Mach number ~ 2 (for Carbon), see Fig. 3. In other words, as soon as the electrons are heated, the ions are heated as well to the temperatures generally speaking exceeding the electron temperature, following the general trend reported in Ref. [8].

We now discuss in some more detail our assumption of the “stiffness” of one jet with respect to perturbations in the other jet. Consider an order one density perturbation with a length-scale ℓ in one of the jets. The corresponding electric field perturbation,

which would perturb the ions in the other jet, is $\sim T_e / e\ell$. Within the time $\ell / 2u$ that the perturbation passes through the location of a certain ion, the ion acquires velocity $\sim (ZT_e / m_i \ell) \times (\ell / 2u) \sim s^2 / 2u$. This velocity is much smaller than the sound speed s , which is a characteristic velocity for the “natural” redistribution of ions in the jet. In other words, the presence of even significant perturbation in one jet has only a weak effect on the other jet. We leave a more detailed analysis of the coupled dynamics for the future work.

In summary: The interpenetrating high-speed plasma jets, although they are almost collisionless with respect to collisions between the ions of the two jets can be highly collisional within each jet. The intra-jet dynamics is described by peculiar hydrodynamic equations, with the presence of the second jet entering the problem via the quasi-neutrality constraint due to the presence of a stiff ion background. The properties of acoustic waves and shock waves in this modified hydrodynamics are briefly analyzed. It is shown that, for the conditions of experiments [1, 8], the rapid ion heating observed after the jets overlapped can be explained by the fast electron heating and formation of the modest-intensity intra-jet shocks by the overtaking effect.

The authors are grateful to W.J. Rozmus for helpful discussion. Work performed for U.S. DoE by LLNL under Contract DE-AC52-07NA27344.

References

1. Hye-Sook Park, D.D. Ryutov, J.S. Ross, N.L. Kugland, et al. “Studying astrophysical collisionless shocks with counterstreaming plasmas from high power lasers,” *High Energy Density Physics*, **8**, 38, January 2012.
2. L. Romagnani, S.V. Bulanov, M. Borghesi, P. Audebert, et al. “Observation of Collisionless Shocks in Laser-Plasma Experiments.” *Phys. Rev. Lett.*, **101**, 025004 (2008).
3. Kuramitsu Y.; Sakawa Y.; Morita T.; et al. “Time Evolution of Collisionless Shock in Counterstreaming Laser-Produced Plasmas.” *Phys. Rev. Lett.* 106, 175002 (2011).
4. Liu X.; Li Y. T.; Zhang Y.; et al, Collisionless shockwaves formed by counterstreaming laser-produced plasmas.” *New Journal of Physics*, **13**, 093001 (2011)
5. M.V. Medvedev, O.V. Zakutnyaya. *Astrophys. J.* **696**, 2269 (2009)
6. A. Spitkovsky, *Astrophys. J.* **698**, 1523 (2009).
7. R. P. Drake, G. Gregori. *Astrophys. J.* **749**, 171 (2012)
8. J. S. Ross, S. H. Glenzer, et al. “Characterizing counter-streaming interpenetrating plasmas relevant to astrophysical collisionless shocks.” *Phys. Plasmas*, **19**, 056501 (2012)
9. D.D. Ryutov, N.L. Kugland, H.-S. Park, S.M. Pollaine, B.A. Remington, J.S. Ross. *Phys. Plasmas*, **18**, 104504 (2011)
10. S.I. Braginski, “Transport Processes in a Plasma,” In: *Reviews of Plasma Physics*, M.A. Leontovich, Ed. Consultants Bureau, New York, 1965
11. S. I. Krasheninnikov. *Phys. Fluids* **B5**, 74 (1993)

12. L.D. Landau, E.M. Lifshitz. "Fluid Mechanics." Pergamon Press, Oxford – New York – Sydney – Tokyo, 1987.
13. V.I. Karpman. "Non-Linear Waves in Dispersive Media." Pergamon Press, Oxford – New York - Toronto – Sydney, 1975.

TABLE 1 Collisionality and other characteristics of two symmetric counter-propagating jets (Assumptions: fully ionized carbon jets, $Z=6$; ion density per jet 10^{18} cm^{-3} ; velocity of each jet $u=10^8 \text{ cm/s}$; electron and ion temperatures $T_e = T_i=100 \text{ eV}$ before fast electron heating; electron temperature $T_e = 1 \text{ keV}$ after the fast electron heating, length-scale $\ell = 1 \text{ mm}$)

	Inter-jet ion m.f.p.	Intra-jet ion m.f.p.	Electron-ion m.f.p.	$\tau_\chi = \ell^2 / 2\chi_e$	τ_{ee}	Electron Debye radius	Sound-crossing time, ℓ / s
$T_e=T_i=100 \text{ eV}$	10 cm	0.3 μm	4 μm	10 ns	0.004 ns	0.1 μm	10 ns
$T_e=1 \text{ keV}, T_i=300 \text{ eV}$	10 cm	3 μm	400 μm	0.03 ns*	0.12 ns	0.3 μm	2.5 ns
$T_e=1 \text{ keV}, T_i=1 \text{ keV}$	10 cm	30 μm	400 μm	0.03 ns*	0.12 ns	0.3 μm	2 ns

* These numbers are given for reference only, as the standard heat conduction model becomes too inaccurate for $\lambda_{ei} \sim 0.4\ell$ [11]. Note that τ_{ee} (next column) is very short compared to the hydrodynamic times.

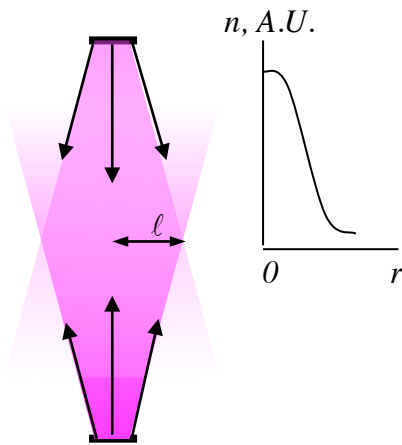


Fig. 1 Two modestly diverging jets formed on planar targets facing each other. The time when significant overlap has already occurred is shown. The right panel is a sketch of the radial density distribution in the mid-plane. After rapid electron heating, the shock can be formed in the zone of the steepest radial gradient.

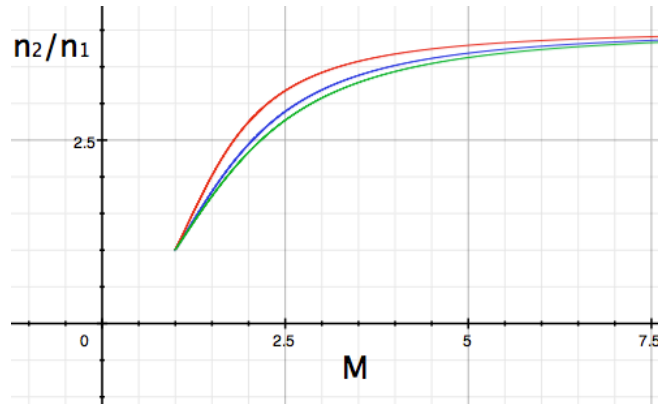


Fig. 2 Compression ratio vs. the Mach number for three values of the parameter $S \equiv n_i/n^*$:

$S = \infty$ (upper curve); $S = 1$ (middle curve); $S = 0.5$ lower curve. Initial ion temperature is

zero.

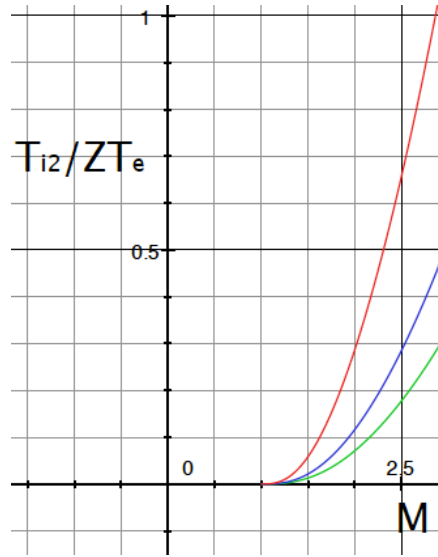


Fig.3 Post-shock ion temperature vs. the Mach number for three values of the parameter $S \equiv n_i/n_e^*$: $S = \infty$ (upper curve); $S = 1$ (middle curve); $S = 0.5$ lower curve. Initial ion temperature is zero. For $S = 1$ and modest shock strengths, $M \sim 2.5$, the ion temperature is $\sim 0.3ZT_e$, i.e., somewhat higher than T_e for carbon.